

## Exploring the Reduction Mechanism of $^{99}\text{Tc(VII)}$ in $\text{NaClO}_4$ : A Spectro-Electrochemical Approach

Rodriguez Hernandez, D. M.; Mayordomo, N.; Parra-Puerto, A.; Schild, D.; Brendler, V.; Stumpf, T.; Müller, K.;

Originally published:

June 2022

**Inorganic Chemistry 61(2022)26, 10159-10166**

DOI: <https://doi.org/10.1021/acs.inorgchem.2c01278>

Perma-Link to Publication Repository of HZDR:

<https://www.hzdr.de/publications/Publ-34883>

Release of the secondary publication  
on the basis of the German Copyright Law § 38 Section 4.

# 1 Exploring the reduction mechanism of $^{99}\text{Tc(VII)}$ in 2 $\text{NaClO}_4$ : A spectro-electrochemical approach

3  
4 *Diana M. Rodríguez*<sup>1</sup>, *Natalia Mayordomo*<sup>1\*</sup>, *Andrés Parra-Puerto*<sup>2</sup>, *Dieter Schild*<sup>3</sup>, *Vinzenz Brendler*  
5 *<sup>1</sup>, Thorsten Stumpf*<sup>1</sup>, *Katharina Müller*<sup>1\*</sup>

6  
7 <sup>1</sup> Institute of Resource Ecology, Helmholtz-Zentrum Dresden – Rossendorf e.V., Bautzner Landstraße  
8 400, 01328 Dresden, Germany.

9 <sup>2</sup> Department of Chemistry, Imperial College London, London, SW7 2AZ, United Kingdom.

10 <sup>3</sup> Institute for Nuclear Waste Disposal, Karlsruhe Institute of Technology (KIT), Hermann-von-  
11 Helmholtz-Platz 1, 76344 Eggenstein-Leopoldshafen, Germany.

12 \* Corresponding authors: [n.mayordomo-herranz@hzdr.de](mailto:n.mayordomo-herranz@hzdr.de) (N. Mayordomo, Phone: +49 351 260 2076),  
13 [k.mueller@hzdr.de](mailto:k.mueller@hzdr.de) (K. Müller, Phone: +49 351 260 2439)

## 14 15 ABSTRACT

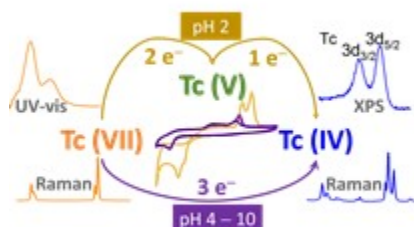
16 Technetium (Tc) is an environmentally relevant radioactive contaminant whose migration is limited  
17 when Tc(VII) is reduced to Tc(IV). However, its reaction mechanisms are not well understood yet. We  
18 have combined electrochemistry, spectroscopy, and microscopy (cyclic voltammetry, rotating disk  
19 electrode, X-ray photoelectron spectroscopy, Raman and scanning electron microscopy) to study Tc(VII)  
20 reduction in non-complexing media: 0.5 mM  $\text{KTcO}_4$  in 2 M  $\text{NaClO}_4$  in the pH from 2.0 to 10.0. At pH  
21 2.0, Tc(VII) first gains  $2.3 \pm 0.3$  electrons, following Tc(V) rapidly receives  $1.3 \pm 0.3$  electrons yielding  
22 Tc(IV). At pH 4.0-10.0, Tc(IV) is directly obtained by transfer of  $3.2 \pm 0.3$  electrons. The reduction of  
23 Tc(VII) produced always a black solid identified as Tc(IV) by Raman and XPS. Our results narrow a  
24 significant gap in the fundamental knowledge of Tc aqueous chemistry and are important to understand  
25 Tc speciation. They provide basic steps on the way from non-complexing to complex media.

26

27

28 SYNOPSIS

29 The reduction of Tc(VII) to Tc(IV) in non-complexing media depends on pH. At pH 2, Tc(VII) gains  
30 two electrons and consequently Tc(V) gains an additional electron to become Tc(IV); whereas at pH 4-  
31 10 Tc(VIII) reduces directly to Tc(IV).



32

33 KEYWORDS:

34 Technetium • Raman spectroscopy • X-ray photoelectron spectroscopy • Non-complexing media •  
35 Electrochemistry • Electron transfer

36

37 1. INTRODUCTION

38 Technetium (Tc, Z=43), discovered by Sagré and Perrier in 1937<sup>1</sup>, is the lightest element with no  
39 stable isotopes. Among them, the most abundant is <sup>99</sup>Tc, a β-particle emitter with a long half-life of  
40 2.14×10<sup>5</sup> years. In the early 60s the application as clinical tracer of the metastable isotope, <sup>99m</sup>Tc (half-  
41 life of 6.007 h), was first published<sup>2</sup> and, since then, it has been used for the imaging of several organs  
42 like the brain and the lungs.

43

44 Technetium might occur naturally within the Earth crust originating from spontaneous fission of <sup>238</sup>U,  
45 neutron-induced fission of <sup>235</sup>U, or interactions between molybdenum, ruthenium or niobium and cosmic  
46 rays<sup>3</sup>. However, the vast majority of the <sup>99</sup>Tc found on Earth is a result of anthropogenic activity such  
47 as nuclear energy production and nuclear weapon testing<sup>3,4</sup>, as well as the decay product of <sup>99m</sup>Tc used  
48 in diagnostics<sup>5,6</sup>. In a typical 1 GW nuclear power plant, 21 kg of <sup>99</sup>Tc (13.2×10<sup>15</sup> Bq) are formed  
49 annually as fission product<sup>7</sup>; the global Tc production in 2007 was estimated to be 15.1×10<sup>3</sup> kg. Taking  
50 this as a rough average, in 2020 there were approximately 4.71×10<sup>5</sup> kg <sup>99</sup>Tc, equivalent to 2.963×10<sup>17</sup> Bq,  
51 present on Earth. The majority of Tc waste is still waiting for proper disposal in deep geological  
52 repositories that, combining engineered (e.g. vitrified waste, buffer and sealing materials, borehole

53 fillings) and geological barriers (host-rock) will isolate the radioactive waste from the (hydro)biosphere  
54 for up to one million years <sup>7</sup>.

55 To ensure a safe storage, it is of utmost importance to understand Tc chemical behavior to assess its  
56 migration in water, which is strongly influenced by its aqueous speciation <sup>8</sup>. Under oxidizing conditions  
57 it occurs as pertechnetate,  $\text{Tc(VII)O}_4^-$ , an anion with high water solubility and low to no interaction with  
58 geochemical barriers <sup>9,10</sup>. Consequently, an ingress of ground water to the repository under oxidizing  
59 conditions – as worst case scenario – will trigger the migration of Tc(VII) to the biosphere. There, it  
60 could easily get incorporated into the food chain causing health problems to animals and humans <sup>3,7,11</sup>.  
61 Under reducing conditions, Tc(IV) is the most stable oxidation state, which commonly forms a solid,  
62  $\text{TcO}_2$ , with a low aqueous solubility ( $\log K_{\text{sp}} = 8.17 \pm 0.05$  <sup>12</sup>). Thus, the reduction of Tc(VII) to Tc(IV)  
63 is an effective strategy for technetium immobilization. Recently several Fe(II) minerals have been studied  
64 in detail: Iron sulfide in the form of pyrite and marcasite <sup>13–15</sup> chukanovite, <sup>16</sup> magnetite <sup>17,18</sup>, or other  
65 common systems like layered double hydroxides <sup>19</sup> trigger Tc(VII) reduction and then incorporate,  
66 precipitate or adsorb Tc(IV).

67 Despite the clear relevance of the reduction of Tc(VII) from an environmental and chemical point of  
68 view, more than 80 years after the discovery of technetium, its reduction mechanisms in water are not  
69 well understood yet <sup>20</sup>. Although several studies have been performed, especially in acidic media <sup>21–23</sup>, it  
70 is not clear whether it proceeds in a direct three-electron transfer or if there are intermediary oxidation  
71 states involved <sup>24–26</sup>. Moreover, there is no systematic study of the effect of pH and ionic strength on the  
72 mechanism. There are also some contradictions observed in the literature. For example, Salaria et al. <sup>27,28</sup>  
73 propose the reduction from Tc(VII) to Tc(III) passing through Tc(IV), whereas Grassi et al. <sup>29</sup> propose  
74 the reduction from Tc(VII) to Tc(IV) with the direct transfer of three electrons, and other authors suggest  
75 that the final product would be Tc(IV) with Tc(V) as an intermediary step <sup>30–32</sup>. Moreover, it must be  
76 noted that all these previous studies use ions like  $\text{Cl}^-$  as background electrolytes that are well known to  
77 form complexes with technetium <sup>12,33</sup>, invalidating such results for a formulation of redox mechanisms  
78 in pure water. This seriously hampers the modeling of technetium migration behavior in any  
79 compartment of geosphere or ecosphere.

80

81 In order to narrow this substantial gap in the understanding of technetium aqueous chemistry, we studied  
82 the reduction of Tc(VII) in sodium perchlorate ( $\text{NaClO}_4$ ), a stable background electrolyte that does not  
83 form complexes with Tc(VII) <sup>12</sup> and, in consequence, minimizes artefacts in reactive transport models  
84 for Tc in aqueous media. This will provide valuable reference data for more complex systems in the

85 future. Experiments were performed at  $2.0 \leq \text{pH} \leq 10.0$  in order to determine the effect of pH on the  
86 mechanism and the reaction products. To get comprehensive molecular understanding on the Tc  
87 reduction chemistry, we combined electrochemical (cyclic voltammetry and rotating disk electrode),  
88 spectroscopic (Raman and X-ray photoelectron spectroscopy), and microscopic (scanning electron  
89 microscopy) methods.

90  
91

## 92 **2. MATERIALS AND METHODS**

### 93 **2.1 Sample preparation**

94 **Radiation safety.**  $^{99}\text{Tc}$  is a  $\beta$ -particle emitter and should be handled only in a dedicated radiochemistry  
95 laboratory with specific radiation safety measurements in place.

96 All solutions were prepared using  $\text{K}^{99}\text{TcO}_4$  (Institute of Radiopharmaceutical Cancer Research at  
97 Helmholtz-Zentrum Dresden-Rossendorf),  $\text{NaClO}_4 \times \text{H}_2\text{O}$  (purity  $\geq 98\%$ , PanReac AppliChem ITW  
98 Reagents) and Milli-Q water (resistivity of  $18.2 \text{ M}\Omega \text{ cm}$ , Water Purified®). In general, 7 mL of 0.5 mM  
99  $\text{KTcO}_4$  solutions were prepared in 2 M  $\text{NaClO}_4$  at pH 2.0, 4.0, 6.0, 8.0, 10.0. The concentrations of both  
100  $\text{NaClO}_4$  and  $\text{KTcO}_4$  were constant throughout the experiments. The pH was adjusted by adding small  
101 amounts (less than  $10 \mu\text{L}$  in total) of  $\text{HClO}_4$  or  $\text{NaOH}$ , changes in ionic strength and viscosity were  
102 negligible. The pH was measured using a pH meter (pH3110, WTW) with a pH electrode (SI Analytics  
103 Blue Line) calibrated with standard pH buffers 4.006, 6.865 and 9.180 (WTW).

104

### 105 **2.2 Cyclic voltammetry (CV) and rotating disk electrode (RDE)**

106 The CV and RDE experiments were performed in an 884 Professional VA instrument from Metrohm  
107 using a three-electrode set-up consisting in a glassy carbon electrode (diameter:  $2 \pm 0.1 \text{ mm}$ ) as working  
108 electrode (WE), platinum as counter electrode (CE) and an  $\text{Ag}/\text{AgCl}$  (3 M  $\text{KCl}$ ) reference electrode (RE);  
109 all potentials were converted to reversible hydrogen electrode (RHE). The electrochemical surface area  
110 of the working electrode was determined as  $0.035 \pm 0.001 \text{ cm}^2$  with a Randles-Sevcik analysis of 10 mM  
111  $\text{K}_3\text{Fe}(\text{CN})_6$  in 1.0 M  $\text{KNO}_3$  using the diffusion coefficients reported on reference <sup>34</sup>. The glassy carbon  
112 electrode was used in stationary mode for CV and in hydrodynamic mode for RDE. The experiments  
113 were performed under normal atmosphere at  $25^\circ\text{C}$  and all the solutions were purged with  $\text{N}_2$  for 20  
114 minutes before the measurement. The data obtained with the RDE were processed with the software  
115 AfterMath (version 1.5.9888, Pine Research) in order to obtain the limiting currents at the different  
116 angular velocities.

117

### 118 **2.3 Spectro-electrochemical analysis**

119 Figure S1 in the Supporting Information presents the in-house-built spectro-electrochemical cell. The  
120 cell was placed inside a glovebox (GS Glovebox-System GS050912; < 1 ppm O<sub>2</sub>) represented by the  
121 orange-colored line in the Figure S1a. The cell holder was printed with a 3D printer (3DWOX 1, Sindoh).  
122 The quartz cell had the following outer dimensions: width 20 × depth 10 × height 30 mm and an optical  
123 path length of 5 mm. For the electrochemical reduction of Tc(VII) a three-electrode arrangement was  
124 used. The WE was a glassy carbon rod (ALS Japan), the CE was a Pt wire (ALS Japan) and the RE was  
125 Ag/AgCl (3 M KCl) (ALS Japan). The electrodes were connected to a potentiostat (PGSTAT 101,  
126 Metrohm) outside the glovebox. An UV-vis spectrometer (AvaSpec-ULS2048 StarLine, Avantes) was  
127 located outside the glovebox along with the lamp (AvaLight-DH-S-BAL, Avantes) and both of them  
128 were connected to the cell holder using optical fiber.

129 The spectro-electrochemical experiments were carried out at 21°C. As general procedure, the sample  
130 was placed inside the cell and it was stirred throughout the entire experiment with a 5 mm magnetic  
131 stirrer. A potential staircase was applied varying the potential 0.01 V every four minutes (for example:  
132 -0.480 V for four minutes, then -0.490 V again for four minutes and so forth until -1 V vs Ag/AgCl or  
133 -0.790 V vs RHE). The starting potential of the staircase was -0.490 V vs Ag/AgCl at pH 2.0 and -0.620  
134 V vs Ag/AgCl at pH 10.0. In parallel to the potential staircase, UV-vis spectra were continuously  
135 recorded (one spectrum every 30 seconds, i.e. 8 spectra per potential value) in the range from 200 to  
136 1100 nm. The integration time was 10 ms and a background subtraction was performed using blanks of  
137 2 M NaClO<sub>4</sub> at pH 2.0 and 10.0 depending on the sample. The 8 spectra obtained for each potential step  
138 were averaged in order to reduce the noise.

### 139 **2.4 Solid analysis**

140 After the complete reduction of Tc(VII) in the spectro-electrochemical cell at pH 2.0, a black solid was  
141 accumulated on the working electrode. The electrode was taken outside the solution and, when it got dry,  
142 the solid detached itself immediately and was collected for further study. The reduction in the spectro-  
143 electrochemical cell was repeated at pH 10.0 obtaining again a solid accumulated on the electrode that  
144 was also harvested. Both solid samples were studied by Raman microscopy, with a second batch of the  
145 solid obtained at pH 2.0 also being analyzed using scanning electron microscopy with energy dispersive  
146 X-ray spectroscopy (SEM-EDX) and X-ray photoelectron spectroscopy (XPS). Experimental conditions  
147 for Raman measurements<sup>35</sup> and for SEM-EDX and XPS<sup>15</sup> are described elsewhere and detailed in the  
148 supporting information.

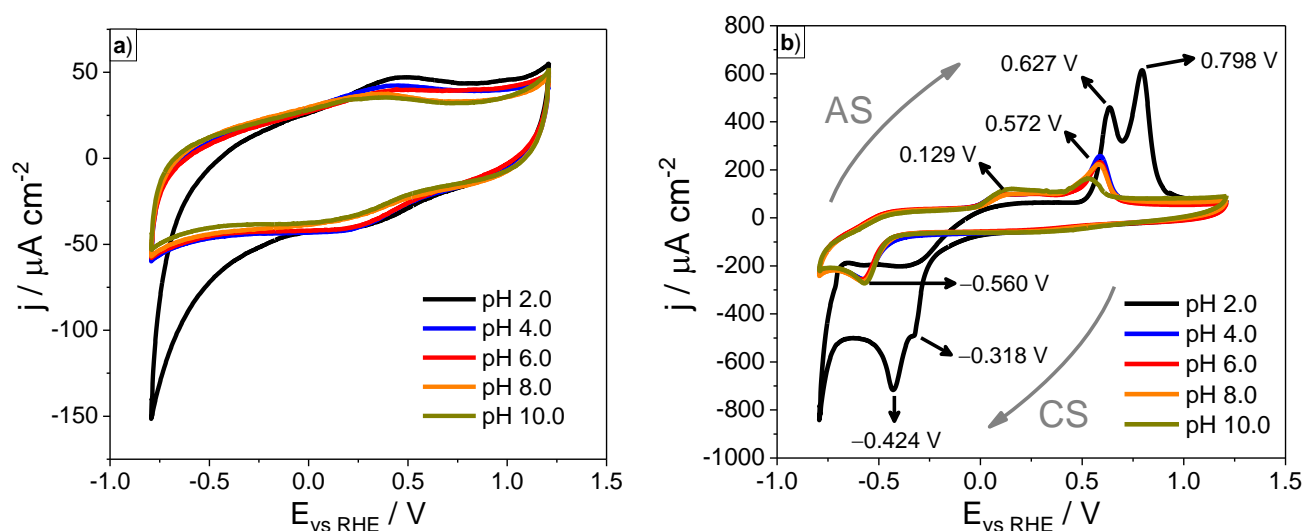
149 The supernatant was analyzed by liquid scintillation counting (1414 LSC Winspectral  $\alpha/\beta$  Wallac, Perkin  
150 Elmer; detection limit: 25 cpm. Measuring time: 10 minutes) finding that only 80 Bq out of the initial  
151 321000 Bq remained in the solution, meaning that all Tc(VII) was reduced to the black Tc solid.  
152

### 153 3. RESULTS AND DISCUSSION

154

#### 155 3.1 Electrochemical Characterization, Cyclic Voltammetry (CV) and Rotating Disk Electrode 156 (RDE)

157 Figure 1 shows the cyclic voltammograms of NaClO<sub>4</sub> solutions in absence (Figure 1a) and presence of  
158 Tc (Figure 1b) in the pH range from 2.0 to 10.0.



159

160 **Figure 1.** Cyclic voltammograms at  $0.01 \text{ V s}^{-1}$  scan rate in 2 M NaClO<sub>4</sub> under N<sub>2</sub> at different pH values a) in  
161 absence of Tc and b) in presence of 0.5 mM KTcO<sub>4</sub>. Grey arrows represent the voltage scan direction of the  
162 cathodic scan (CS) and the anodic scan (AS).

163 As mentioned before, unlike chloride (Cl<sup>-</sup>), perchlorate (ClO<sub>4</sub><sup>-</sup>) does not form complexes with  
164 technetium<sup>12</sup>. In addition to that, the voltammogram of NaClO<sub>4</sub> (Figure 1a) shows only very small peaks  
165 close to 0.1 V vs. reversible hydrogen electrode (RHE) and some hydrogen evolution reaction potentials  
166 below -0.625 V at pH 2.0. In the presence of Tc, the voltammograms clearly change. Thus, the peaks in  
167 Figure 1b indicate the course of different oxidation states of technetium within the cycling  
168 voltammograms.

169 Two different Tc reduction behaviors can be spotted in the CVs depending on the pH in the cathodic  
170 scan. At pH 2.0 the system clearly shows two peaks during the reduction. A small peak at  $-0.318$  V  
171 suggests the formation of an intermediary oxidation state, followed by a second reduction peak observed  
172 at  $-0.424$  V. In contrast, at pH 4.0-10.0 one single cathodic peak at  $-0.560$  V indicates a direct Tc(VII)  
173 reduction.

174

175 The voltammograms in Figure 1b show two anodic peaks despite the pH value, i.e. the formation of two  
176 Tc oxidation states. The potential of the reactions depends on the pH alike the reduction: while at pH 4.0  
177  $- 10.0$  they behave in a similar way (anodic peaks at  $0.129$  V and  $0.570$  V), the peaks at pH 2.0 are shifted  
178 to more positive values ( $0.627$  V and  $0.789$  V).

179

180 Although, the CVs provide already an idea on the mechanism of the Tc reduction and oxidation, they  
181 cannot be used for the determination of the exact amount of electrons transferred, due to the irreversibility  
182 of the process. For an improved understanding of the redox processes occurring, we combine cyclic  
183 voltammetry at different scan rates and the rotating disk electrode technique to apply the Randles-Sevcik  
184 and Levich equations for electrochemical data analysis. A full description of the equations and how to  
185 interpret them is defined as follows.

186 On one hand, by changing the scan rate of the CV, the peak currents can be analyzed with the Randles-  
187 Sevcik equation (Eq. [1])<sup>36,37</sup>. It is assumed that all Tc remains dissolved and there is no precipitation or  
188 deposition on the electrode.

$$189 \quad I_p = 2.69 \times 10^5 n^{3/2} A c D^{1/2} \nu^{1/2} \quad [1]$$

190 where  $I_p$  is the peak current (A),  $n$  is the number of electrons transferred,  $A$  the area of the electrode  
191 ( $\text{cm}^2$ ),  $c$  the analyte concentration ( $\text{mol cm}^{-3}$ ),  $D$  the diffusion coefficient ( $\text{cm}^2 \text{s}^{-1}$ ), and  $\nu$  the CV scan  
192 rate ( $\text{V s}^{-1}$ ). The terms  $n$ ,  $A$ ,  $c$  and  $D$  do not change here and can be grouped along with  $2.69 \times 10^5$  in a  
193 new term  $Y$ . Therefore, Eq. [1] can be rewritten as Eq. [2].

194 When  $I_p$  is plotted vs.  $\nu^{1/2}$  (Randles-Sevcik plot) a straight line with slope  $Y$  is obtained.

$$195 \quad I_p = Y \nu^{1/2} \quad [2]$$

196 On the other hand, using a rotating disk electrode (RDE) the diffusion coefficients and the number of  
197 electrons can be determined. RDE is an experimental technique in which the working electrode rotates



198 on its own axis creating a laminar flow of the solution towards the electrode, improving the mass transport  
199 <sup>38</sup>. Such flow can be controlled by the angular velocity of the electrode and the behavior of the current is  
200 modelled using the Levich equation (Eq. [3]) <sup>38</sup>.

$$201 \quad I_L = (0.620) n F A v^{-1/6} D^{2/3} c \omega^{1/2} \quad [3]$$

202 where  $I_L$  is the limiting current (A), which is the mass transport limited current obtained at the different  
203 rotation speed,  $n$  is the number of electrons transferred,  $F$  the Faraday constant (96 485.3329 C mol<sup>-1</sup>),  
204  $A$  the area of the electrode (cm<sup>2</sup>),  $v$  the kinematic viscosity of the electrolyte (cm<sup>2</sup> s<sup>-1</sup>),  $D$  the diffusion  
205 coefficient of the species under study, i.e. the electroactive species (cm<sup>2</sup> s<sup>-1</sup>),  $c$  the analyte concentration  
206 (mol cm<sup>-3</sup>) and  $\omega$  the angular velocity of the RDE (rads<sup>-1</sup>). Alike Randles-Sevcik equation,  $n$ ,  $A$ ,  $v$ ,  $D$   
207 and  $c$  can be grouped along with 0.620  $F$  in  $B$  (Levich constant) and Eq. [3] can be summarized as Eq.  
208 [4].

$$209 \quad I_L = B \omega^{1/2} \quad [4]$$

210 When plotting  $I_L$  vs.  $\omega^{1/2}$  (Levich plot)  $B$  is obtained from the slope of a linear fit and is used to determine  
211 the number of electrons transferred  $n$  or the diffusion coefficient  $D$ . In our system, we have approximated  
212  $v$  by  $8.90 \times 10^{-3}$  cm<sup>2</sup> s<sup>-1</sup> corresponding to the kinematic viscosity of 2 M NaClO<sub>4</sub> in water <sup>39</sup>. The Tc  
213 concentration (0.5 mM) was low enough to neglect its effect on the viscosity.

214 Combining the slopes of the regression lines from the Randles-Sevcik and the Levich equations, two  
215 equations (Eq. [5] and Eq. [6]) are obtained for two unknown variables ( $D$  – the diffusion coefficient of  
216 Tc in 2 M NaClO<sub>4</sub> and  $n$ ):

$$217 \quad Y = 2.69 \times 10^5 A c D^{1/2} n^{3/2} \quad [5]$$

$$218 \quad B = 0.620 F c A v^{-1/6} D^{2/3} n \quad [6]$$

219 Solving this equation system, Eq. [7] and [8] were obtained, directly yielding  $D$  and  $n$ , respectively:

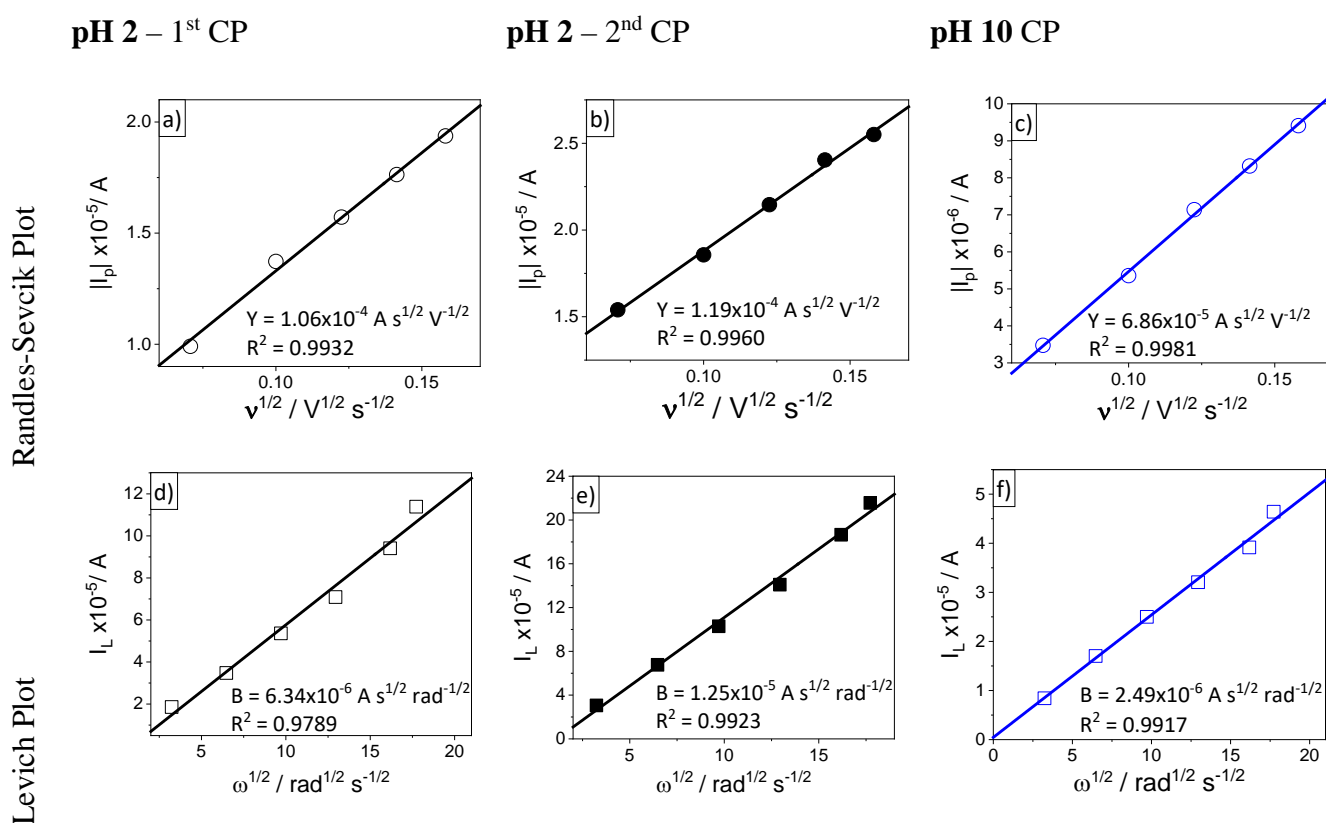
$$220 \quad D = \left( \frac{\alpha E}{B} \right)^2 \quad [7]$$

$$221 \quad n = \frac{Y}{\alpha D^{3/2}} \quad [8]$$

222 with  $\alpha = 0.620 F c A v^{-1/6}$ ,  $E = (Y/\beta)^{3/2}$  and  $\beta = 2.69 \times 10^5 A c$ .

223 Since the reduction of Tc(VII) in NaClO<sub>4</sub> appears to follow the same mechanism throughout the pH  
 224 range 4.0-10.0 according to Figure 1b, we selected pH 2.0 and pH 10.0 for the RDE experiments to  
 225 encompass the working pH range by measuring the two extremes. The reduction curves of the systems  
 226 at different angular velocities as well as the cyclic voltammograms at different scan rates are presented  
 227 in Figures S2 and S3 in the supporting information. Figure 2 shows the Randles-Sevcik and Levich plots  
 228 of Tc at pH 2.0 and 10.0. There is a clear linear correlation between  $I_L$  and  $\omega^{1/2}$  as well as for  $I_p$  and  $u^{1/2}$ ,  
 229 and, therefore, the values for the slopes  $B$  and  $Y$  were replaced in Eq. [5] and [6] to obtain  $D$  and  $n$  at  
 230 both pH values.

231 Table 1 summarizes the results of the electrochemical analysis.



232 **Figure 2.** (circles) Randles-Sevcik and (squares) Levich plots of 0.5 mM KTcO<sub>4</sub> in 2 M NaClO<sub>4</sub> at different pH  
 233 values. a), d) First cathodic peak (CP) at pH 2.0 (–0.318 V). b), e) Second cathodic peak (CP) at pH 2.0 (–0.424  
 234 V) c), f) Cathodic peak at pH 10.0 (–0.560 V).  $Y$  and  $B$  are the Randles-Sevcik and Levich slopes (Eq. [5] and [6]  
 235 respectively).

236

237 **Table 1.** Reduction mechanism of Tc(VII) in NaClO<sub>4</sub> at pH 2.0 and pH 4.0-10.0 in their respective  
 238 cathodic peaks (CP) and the associated reduction potential vs reversible hydrogen electrode (E<sub>vs RHE</sub>).

	pH 2.0	4.0-10.0
CP		
	Tc(VII) + 2.3 ± 0.3 e <sup>-</sup> → Tc(V)	Tc(VII) + 3.2 ± 0.3 e <sup>-</sup> → Tc(IV)
1	D = 3.92×10 <sup>-5</sup> cm <sup>2</sup> s <sup>-1</sup>	D = 5.75×10 <sup>-6</sup> cm <sup>2</sup> s <sup>-1</sup>
	E <sub>vs RHE</sub> = -0.318 V	E <sub>vs RHE</sub> = -0.560 V
	Tc(V) + 1.3 ± 0.3 e <sup>-</sup> → Tc(IV)	
2	D = 2.41×10 <sup>-4</sup> cm <sup>2</sup> s <sup>-1</sup>	----
	E <sub>vs RHE</sub> = -0.424 V	

239 *n* and *D* were calculated with Equations [7] and [8].

240 We have found that at pH 2.0 the reduction of Tc(VII) begins with the transfer of 2.3 ± 0.3 electrons  
 241 yielding Tc(V) as an intermediary oxidation state that subsequently gains further 1.3 ± 0.3 electrons to  
 242 become Tc(IV). At pH 10.0, the reduction of Tc(VII) is direct with the transfer of 3.2 ± 0.3 electrons to  
 243 produce Tc(IV). The uncertainties in the number of errors were calculated using the error propagation  
 244 method described elsewhere<sup>40</sup>.

245 The electrochemical behavior displayed at pH 2.0 is in good agreement with the Latimer diagram of Tc  
 246 under acidic conditions<sup>41</sup> where Tc(VI) is postulated as an intermediary oxidation state during the  
 247 reduction from Tc(VII) to Tc(IV). However, as Tc(VI) is unstable in water, a rapid disproportionation to  
 248 Tc(VII) and Tc(V) takes place<sup>25,27,29</sup>. This supports the electrochemical analysis (Table 1), suggesting  
 249 that the small peak at -0.318 V at pH 2.0 is Tc(V). The potential shift with pH related to Tc(IV) formation  
 250 (-0.424 V for pH 2 and -0.560 V for pH values 4.0, 6.0, 8.0 and 10.0) can be related to the difference in  
 251 the pH, as it occurs, for example, with manganese where the reduction from Mn(VII)O<sub>4</sub><sup>-</sup> to Mn(IV)O<sub>2</sub>  
 252 has a standard potential of 1.7 V at acidic pH and 0.60 V at alkaline pH, according to Mn Latimer  
 253 diagrams<sup>25</sup>.

254 The diffusion coefficients of the electroactive Tc species in NaClO<sub>4</sub> at pH 2.0 were determined as  
 255 3.92×10<sup>-5</sup> cm<sup>2</sup> s<sup>-1</sup> for Tc(VII) and 2.41×10<sup>-4</sup> cm<sup>2</sup> s<sup>-1</sup> for Tc(V). At pH 10.0, the diffusion coefficient of  
 256 Tc(VII) is 5.75×10<sup>-6</sup> cm<sup>2</sup> s<sup>-1</sup>. The starting Tc oxidation state at both pH 2.0 and pH 10.0 is Tc(VII), and,  
 257 therefore, it is clear that pertechnetate is the electroactive species of the first cathodic peaks (CP) at both  
 258 pH values. Previous studies on Tc diffusion coefficients in aqueous solution are extremely limited and  
 259 no value could be found in the presence of a salt that remotely resembles NaClO<sub>4</sub> (like KClO<sub>4</sub> or

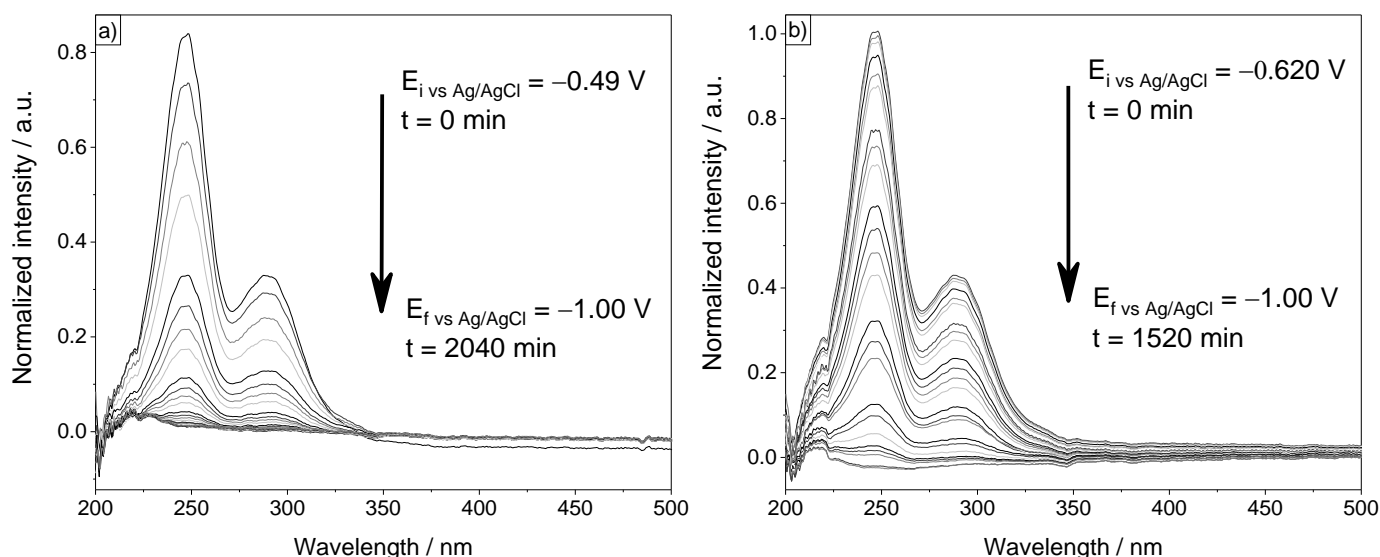
260 NaBrO<sub>4</sub>). For the sake of comparison the values obtained in our work were contrasted against the  
261 diffusion coefficients of Tc in bentonite <sup>42</sup>, where it was reported that the diffusion coefficient of  
262 pertechnetate decreases as pH increases, which is in well agreement with our findings with the RDE for  
263 the reduction mechanism of Tc(VII) (Table 1).

264 The oxidation mechanism could not be established because it was not possible to stabilize the reduced  
265 Tc aqueous species –theoretically Tc(IV)– at the begin of the experiment. As it will be shown in section  
266 *Solid Analysis*, the complete reduction of Tc(VII) led to the formation of a solid deposited on the working  
267 electrode (WE), making it impossible to apply the electrochemical analysis presented in this section as it  
268 is only feasible for species in solution. It is worth explaining that this issue did not affect the  
269 determination of the reduction mechanism because both the RDE and the CV experiments were fast  
270 enough to avoid the precipitation of the reduced Tc. However, the complete reduction of Tc(VII)  
271 necessary to start the RDE experiment for the oxidation takes several hours, giving enough time for the  
272 deposition of the reduced Tc solid. However, we can interpret that the second anodic peak (0.798 V at  
273 pH 2.0 and around 0.570 V at pH 4.0 – 10.0) in Figure 1b corresponds to the formation of Tc(VII), as  
274 this is the highest stable oxidation state in solution for technetium

275

### 276 **3.2 In-situ spectro-electrochemical analysis of the Tc(VII) reduction**

277 Spectro-electrochemical experiments were performed to follow the electrochemical reduction of  
278 Tc(VII)O<sub>4</sub><sup>-</sup> in NaClO<sub>4</sub> at both pH 2.0 and 10.0. The collected UV-vis spectra are shown in Figure 3. As  
279 expected, both spectral data sets display at the beginning of the experiments the characteristic signals of  
280 TcO<sub>4</sub><sup>-</sup> at 247 and 289 nm <sup>24</sup>. With the application of the potential staircase, the intensity of these features  
281 gradually decreases until both bands finally disappear at the last potential steps, indicating full reduction  
282 of Tc(VII). The process was identical at both pH 2.0 and 10.0 (Figure 3 a and b).



283 **Figure 3.** UV-vis spectra measured during the electrochemical reduction of 0.5 mM  $\text{Tc(VII)O}_4^-$  in 2 M  $\text{NaClO}_4$ .  
 284 a) pH 2.0. b) pH 10.0.

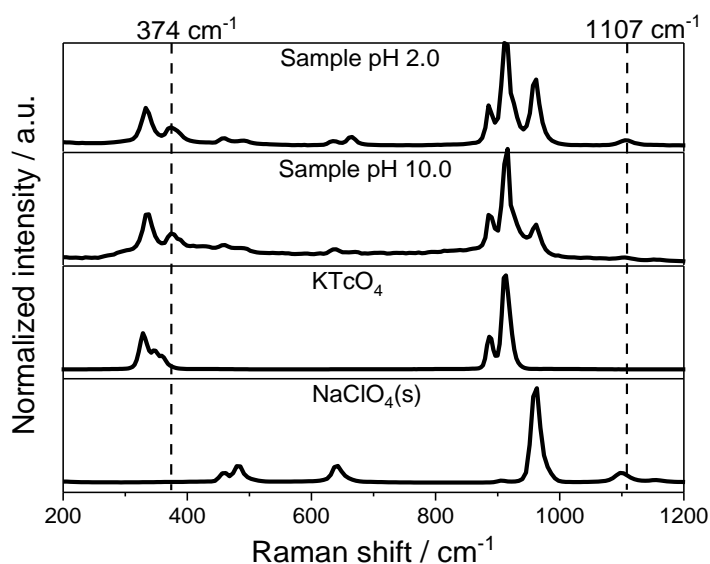
285 The complete reduction of  $\text{Tc(VII)}$  yielded a black solid deposited on the WE regardless of the sample  
 286 pH. Taking into account, that UV-vis spectra confirm the lack of  $\text{Tc(IV)}$  chloride species with absorption  
 287 at 234 nm and 338 nm<sup>43</sup>, and that  $\text{Tc(IV)}$  is the final reduction product (Table 1), most likely the formed  
 288 solid is a  $\text{Tc(IV)-O}$  species.

289 The spectroscopic behavior depicted in Figure 3b is in good agreement with the findings of the  
 290 electrochemical analysis at pH 10.0 with no intermediary oxidation state between  $\text{Tc(VII)}$  and  $\text{Tc(IV)}$   
 291 during the reduction. Therefore, the occurrence of a Tc signal different from those of  $\text{Tc(VII)}$  was not  
 292 expected. However, no spectroscopic evidence of the existence of the  $\text{Tc(V)}$  species suggested by the  
 293 electrochemical analysis at pH 2.0 was found. This can be due to an extremely fast transition from  $\text{Tc(V)}$   
 294 to  $\text{Tc(IV)}$  or simply because the  $\text{Tc(V)}$  species is not active in the UV-vis range or its absorption  
 295 coefficient is too low.

296

### 297 3.3 Solid analysis

298 In order to confirm the chemical identity of the solid obtained after the complete reduction of  $\text{Tc(VII)O}_4^-$ ,  
 299 Raman spectroscopy, XPS and SEM-EDX were performed. The Raman spectra of the solids at pH 2.0  
 300 and 10.0 are shown in Figure 4.



301

302 **Figure 4.** Raman spectra of the black solid obtained after the total reduction of 0.5 mM  $\text{KTcO}_4$  in 2 M  $\text{NaClO}_4$  at  
 303 pH 2.0 and 10.0 in the spectro-electrochemical cell. The Raman spectra of  $\text{KTcO}_4$  and  $\text{NaClO}_4$  have been added  
 304 for comparison.

305

306 It can be observed that the Raman spectra are identical for both samples, indicating that the chemical  
 307 identity of the solids at both pH values is the same, supporting the results in Table 1. The spectra of the  
 308 samples were compared with the spectra of  $\text{KTcO}_4$  and  $\text{NaClO}_4$ . The bands at 458, 632, 666 and 960  $\text{cm}^{-1}$   
 309 were attributed to sodium perchlorate<sup>44</sup> recrystallized on the working electrode along with the  
 310 technetium solid.

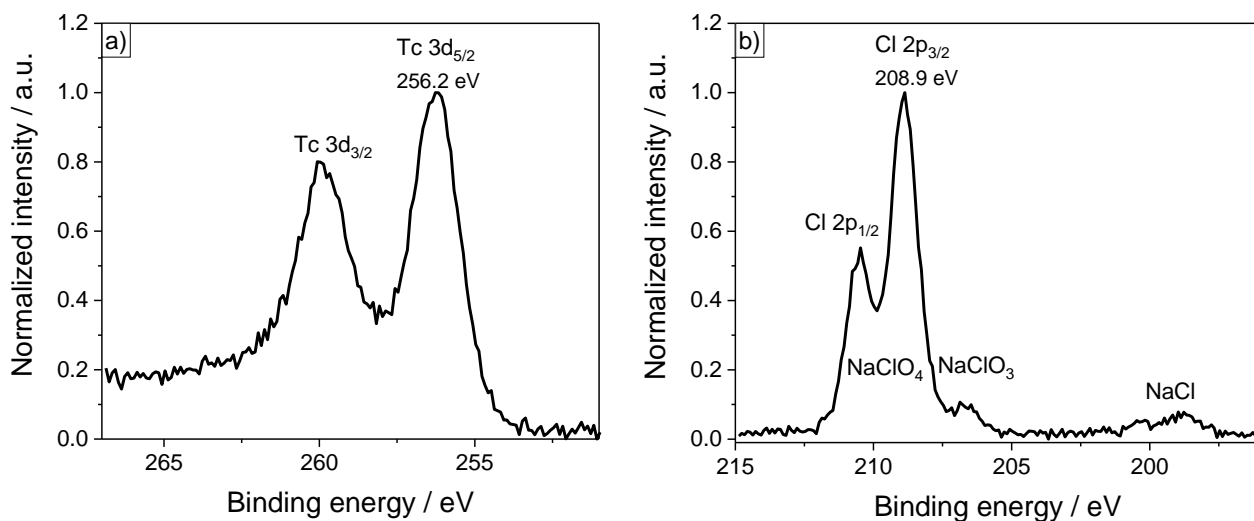
311 The band at 330  $\text{cm}^{-1}$  is assigned to Tc-O vibrations by comparison with the  $\text{KTcO}_4$  spectra<sup>45,46</sup>.  
 312 However, it is worth mentioning that according to the literature<sup>43,47,48</sup> the Tc-Cl bond presents two bands  
 313 at 332 and 342  $\text{cm}^{-1}$ . While no band around 340  $\text{cm}^{-1}$  is present in the spectra of the samples, the bands  
 314 appearing at 885 and 913  $\text{cm}^{-1}$  are characteristic of the  $\text{TcO}_4^-$  structure corresponding to Tc-O vibrations  
 315<sup>45,46</sup>. Therefore, the band at 330  $\text{cm}^{-1}$  is also assigned to the Tc-O vibration and no evidence of Tc-Cl  
 316 bonding is present in the Raman spectra. This confirms that no interaction between Tc and chlorine  
 317 species took place during the reduction.

318 Two bands at 374 and 1107  $\text{cm}^{-1}$  remain unidentified after this assignment. Since the initial components  
 319 of the samples were  $\text{KTcO}_4$ ,  $\text{NaClO}_4$  and water, these two remaining bands can be tentatively assigned  
 320 to the reduced Tc solid that would be Tc(IV) according to the electroanalysis (Table 1). Previous works

321 <sup>49,50</sup> have reported a signal at 877 cm<sup>-1</sup> for TcO<sub>2</sub> that does not appear in the Raman spectra of our samples.  
322 There is a possibility that this signal is overlapped by the band at 885 cm<sup>-1</sup> but, as no reports for signals  
323 at 374 and 1107 cm<sup>-1</sup> have been found for TcO<sub>2</sub>, we refrain from characterizing the solid samples as  
324 technetium dioxide.

325 In order to confirm the oxidation state of technetium in the solid, XPS and SEM-EDX were applied. The  
326 XPS spectra of the solid evaluated in Tc 3d and Cl 2p is presented in Figure 5.

327



328 **Figure 5.** XPS spectra of the reduced Tc solid. s) Tc 3d, b) Cl 2p.

329 The Tc 3d spectrum (Figure 5a) shows an intense Tc 3d<sub>5/2</sub> peak at 256.2 eV assigned to Tc(IV) since it  
330 is close to the reference value for TcO<sub>2</sub> (256.8 eV<sup>51</sup>). NaClO<sub>4</sub> was present during the recording of the  
331 XPS spectra of the sample because no further separation or purification of the solid was performed after  
332 the reduction of Tc(VII) (see solid analysis in the experimental section). The Cl 2p<sub>3/2</sub> elemental line of  
333 NaClO<sub>4</sub> is observed at 208.9 eV binding energy in accordance with its reference at 208.9 eV<sup>52</sup>. Since  
334 NaClO<sub>4</sub> degrades under X-ray irradiation and the charge of the sample surface caused by the XPS  
335 measurement will change slowly during degradation, charge referencing of elemental lines is not reliable  
336 if high degradation of NaClO<sub>4</sub> occurs. This was avoided by using monochromatic Al K<sub>α</sub> X-rays, larger  
337 analysis area, and short acquisition time. Small portions of chlorite and chloride, i.e. the degradation  
338 products, are detected at the Cl 2p spectrum (Figure 5b), making the results presented reliable despite the  
339 presence of NaClO<sub>4</sub>.

340 Even though XPS cannot be used to establish the structure of the technetium compound, the oxidation  
341 state can be unequivocally assigned as Tc(IV). Therefore, the bands found at 374 and 1107 cm<sup>-1</sup> in the

342 Raman spectra correspond to Tc(IV). To our knowledge, apart from the band at  $877\text{ cm}^{-1}$  for  $\text{TcO}_2$ <sup>43</sup>, no  
343 other Raman signals for Tc(IV) have been reported before, making the results of this paper very relevant  
344 for the identification of Tc(IV) in other applications, e.g. Tc retention studies by minerals.

345 The SEM-EDX analysis is presented in Figure S4 in the supporting information. The morphology of the  
346 sample depicted in the micrographs shows three regions clearly separated: (1) mainly Na, Cl and O, (2)  
347 almost completely Tc and O and (3) indium from the foil on which the sample was prepared. This is  
348 consistent with the fact that  $\text{ClO}_4^-$  had no interaction with Tc and the solid obtained corresponds only to  
349 a reduced Tc species bonded to O.

#### 350 **4. CONCLUSIONS**

351 The reduction of Tc(VII) in non-complexing media ( $\text{NaClO}_4$ ) has been studied for the first time using  
352 spectro-electrochemical methods and electrochemical analysis, combined with other spectroscopic and  
353 microscopic techniques.

354 The electrochemical results show that the reaction mechanism depends on the pH. By applying Randles-  
355 Sevcik and Levich equations, the number of electrons during electrochemical analysis was determined.  
356 At pH 2.0, the reduction occurs in two steps with the initial gain of  $2.3 \pm 0.3$  electrons by Tc(VII) to  
357 obtain Tc(V), which subsequently receives  $1.3 \pm 0.3$  electrons to form Tc(IV). At pH 4.0-10.0 Tc(VII) is  
358 directly reduced to Tc(IV) with the transfer of  $3.2 \pm 0.3$  electrons. The electrochemical reduction of  
359 Tc(VII) in  $\text{NaClO}_4$  was followed in parallel with UV-vis absorption spectroscopy. Even though no  
360 spectroscopic evidence of intermediate Tc(V) could be obtained, UV-vis showed the absence of Tc(IV)-  
361 chloride species. After the total reduction of Tc(VII) at both pH 2.0 and 10.0, a black solid was formed.  
362 Raman spectroscopy confirmed that both solids had the same chemical identity despite the initial pH  
363 value, whereas SEM-EDX analysis proves that the solid only consists of Tc and O. XPS analysis  
364 identified the solids as Tc(IV) and agrees with the obtained CV results and the electrochemical analysis.

365 In addition to an accurate determination of the electrons transferred in the reduction process depending  
366 on the pH, this study has also yielded two Raman signals at  $374$  and  $1107\text{ cm}^{-1}$  that correspond to the  
367 Tc(IV) species formed after the total reduction of Tc(VII). Such Raman features will be relevant to  
368 specific questions in environmental engineering for the identification of Tc(IV) compounds that are the  
369 products of the reductive immobilization of Tc(VII) by common minerals and could only be identified  
370 by the use of more expensive spectroscopies.



371 This work presents fundamental data to understand Tc redox chemistry and its dependence on pH under  
372 the simplest aqueous conditions, i.e. in a non-complexing media.

373 Both results and methodology applied in the electrochemical analysis will serve as valuable references  
374 for further studies to identify Tc redox chemistry in complex systems, e.g. in presence of inorganic and  
375 organic ligands. These fundamental studies are essential for a realistic and broad picture of the Tc  
376 chemical redox and complexation behavior. A basic Tc chemical understanding will also provide a direct  
377 impact on environment protection by enhancing Tc remediation strategies in contaminated areas as well  
378 as for the safety assessment of nuclear waste repositories.

379 Furthermore, this work is also the first step towards a future development of spectro-electrochemical  
380 techniques. We envision the development of spectro-electrochemistry couplings to characterize the  
381 structure of redox-active species at different oxidation states, which will be helpful not only for Tc but  
382 also for other redox-active elements whose chemical behavior is still to be fully defined.

383

#### 384 **Abbreviations**

385 CE: counter electrode

386 CP: Cathodic peak

387 CV: Cyclic voltammetry

388 RDE: Rotating disk electrode

389 RE: reference electrode

390 RHE: Reversible hydrogen electrode

391 SEM-EDX: Scanning electron microscopy with energy dispersive X-ray spectroscopy

392 WE: working electrode

393 XPS: X-ray photoelectron spectroscopy

394

395 **Supporting Information.** In-house built spectro-electrochemical cell. Reduction curves. CVs at  
396 different scan rates. SEM-EDX. Experimental description of Tc solid analysis.

397

#### 398 **Acknowledgment**

399 We are very grateful to Susana Jiménez and Stephan Weiß for their help in the lab. We acknowledge the  
400 German Federal Ministry for Economic Affairs and Climate Action (former German Federal Ministry of  
401 Economic Affairs and Energy) for the VESPA II joint project (02E11607B).

402

403 **References**

- 404 (1) Perrier, C.; Segrè, E. Radioactive Isotopes of Element 43. *Nature* **1937**, *140* (3535), 193–194.  
405 <https://doi.org/10.1038/140193b0>.
- 406 (2) Herbert, R.; Kulke, P. W.; Shepherd, R. T. H. The Use of Technetium 99m as a Clinical Tracer  
407 Element. *Postgrad. Med. J.* **1965**, *41* (481), 656–662. <https://doi.org/10.1136/pgmj.41.481.656>.
- 408 (3) Meena, A. H.; Arai, Y. Environmental Geochemistry of Technetium. *Environ. Chem. Lett.* **2017**,  
409 *15* (2), 241–263. <https://doi.org/10.1007/s10311-017-0605-7>.
- 410 (4) Momoshima, N.; Sayad, M.; Yamada, M.; Takamura, M.; Kawamura, H. Global Fallout Levels  
411 of <sup>99</sup>Tc and Activity Ratio of <sup>99</sup>Tc/<sup>137</sup>Cs in the Pacific Ocean. *J. Radioanal. Nucl. Chem.* **2005**, *266*  
412 (3), 455–460. <https://doi.org/10.1007/s10967-005-0931-2>.
- 413 (5) Guérin, B.; Tremblay, S.; Rodrigue, S.; Rousseau, J. A.; Dumulon-Perreault, V.; Lecomte, R.; van  
414 Lier, J. E.; Zyuzin, A.; van Lier, E. J. Cyclotron Production of <sup>99m</sup>Tc: An Approach to the Medical  
415 Isotope Crisis. *J. Nucl. Med.* **2010**, *51* (4), 13N-16N.
- 416 (6) Jurisson, S.; Gawenis, J.; Landa, E. R. Sorption of <sup>99m</sup>Tc Radiopharmaceutical Compounds by  
417 Soils. *Health Phys.* **2004**, *87* (4).
- 418 (7) Icenhower, J. P.; Qafoku, N. P.; Zachara, J. M.; Martin, W. J. The Biogeochemistry of  
419 Technetium: A Review of the Behavior of an Artificial Element in the Natural Environment. *Am.*  
420 *J. Sci.* **2010**, *310* (8), 721–752. <https://doi.org/10.2475/08.2010.02>.
- 421 (8) Lear, G.; McBeth, J. M.; Boothman, C.; Gunning, D. J.; Ellis, B. L.; Lawson, R. S.; Morris, K.;  
422 Burke, I. T.; Bryan, N. D.; Brown, A. P.; Livens, F. R.; Lloyd, J. R. Probing the Biogeochemical  
423 Behavior of Technetium Using a Novel Nuclear Imaging Approach. *Environ. Sci. Technol.* **2010**,  
424 *44* (1), 156–162. <https://doi.org/10.1021/es802885r>.
- 425 (9) Lieser, K. H.; Bauscher, C. Technetium in the Hydrosphere and in the Geosphere. I Chemistry of  
426 Technetium and Iron in Natural Waters and Influence of the Redox Potential on the Sorption of  
427 Technetium. *Radiochim. Acta* **1987**, *42*, 205–213.
- 428 (10) Masters-Waage, N. K.; Morris, K.; Lloyd, J. R.; Shaw, S.; Mosselmans, J. F. W.; Boothman, C.;  
429 Bots, P.; Rizoulis, A.; Livens, F. R.; Law, G. T. W. Impacts of Repeated Redox Cycling on  
430 Technetium Mobility in the Environment. *Environ. Sci. Technol.* **2017**, *51* (24), 14301–14310.  
431 <https://doi.org/10.1021/acs.est.7b02426>.
- 432 (11) Corkhill, C. L.; Bridge, J. W.; Chen, X. C.; Hillel, P.; Thornton, S. F.; Romero-Gonzalez, M. E.;  
433 Banwart, S. A.; Hyatt, N. C. Real-Time Gamma Imaging of Technetium Transport through Natural  
434 and Engineered Porous Materials for Radioactive Waste Disposal. *Environ. Sci. Technol.* **2013**,

- 435 47 (23), 13857–13864. <https://doi.org/10.1021/es402718j>.
- 436 (12) Grenthe, I.; Gaona, X.; Plyasunov, A. V.; Rao, L.; Runde, W. H.; Grambow, B.; Konings, R. J.  
437 M.; Smith, A. L.; Moore, E. E. *Second Update on the Chemical Thermodynamics of Uranium,*  
438 *Neptunium, Plutonium, Americium and Technetium*; OECD Nuclear Energy Agency Data Bank:  
439 Boulogne-Billancourt, France, 2020.
- 440 (13) Rodríguez, D. M.; Mayordomo, N.; Scheinost, A. C.; Schild, D.; Brendler, V.; Müller, K.; Stumpf,  
441 T. New Insights on the <sup>99</sup>Tc(VII) Removal by Pyrite: A Spectroscopic Approach. *Environ. Sci.*  
442 *Technol.* **2020**, *54*, 2678–2687.
- 443 (14) Huo, L.; Xie, W.; Qian, T.; Guan, X.; Zhao, D. Reductive Immobilization of Pertechnetate in Soil  
444 and Groundwater Using Synthetic Pyrite Nanoparticles. *Chemosphere* **2017**, *174*, 456–465.  
445 <https://doi.org/10.1016/j.chemosphere.2017.02.018>.
- 446 (15) Rodríguez, D. M.; Mayordomo, N.; Schild, D.; Shams Aldin Azzam, S.; Brendler, V.; Müller, K.;  
447 Stumpf, T. Reductive Immobilization of <sup>99</sup>Tc(VII) by FeS<sub>2</sub>: The Effect of Marcasite.  
448 *Chemosphere* **2021**, *281*, 130904.  
449 <https://doi.org/https://doi.org/10.1016/j.chemosphere.2021.130904>.
- 450 (16) Schmeide, K.; Rossberg, A.; Bok, F.; Shams Aldin Azzam, S.; Weiss, S.; Scheinost, A. C.  
451 Technetium Immobilization by Chukanovite and Its Oxidative Transformation Products : Neural  
452 Network Analysis of EXAFS Spectra. *Sci. Total Environ.* **2021**, *770*, 145334.  
453 <https://doi.org/10.1016/j.scitotenv.2021.145334>.
- 454 (17) Yalçıntaş, E.; Scheinost, A. C.; Gaona, X.; Altmaier, M. Systematic XAS Study on the Reduction  
455 and Uptake of Tc by Magnetite and Mackinawite. *Dalt. Trans.* **2016**, *45* (44), 17874–17885.  
456 <https://doi.org/10.1039/C6DT02872A>.
- 457 (18) Marshall, T. A.; Morris, K.; Law, G. T. W.; Mosselmans, J. F. W.; Bots, P.; Parry, S. A.; Shaw,  
458 S. Incorporation and Retention of <sup>99</sup>Tc(IV) in Magnetite under High pH Conditions. *Environ. Sci.*  
459 *Technol.* **2014**, *48* (20), 11853–11862. <https://doi.org/10.1021/es503438e>.
- 460 (19) Mayordomo, N.; Rodríguez, D. M.; Rossberg, A.; Foerstendorf, H.; Heim, K.; Brendler, V.;  
461 Müller, K. Analysis of Technetium Immobilization and Its Molecular Retention Mechanisms by  
462 Fe(II)-Al(III)-Cl Layered Double Hydroxide. *Chem. Eng. J.* **2021**, *408*, 127265.  
463 <https://doi.org/10.1016/j.cej.2020.127265>.
- 464 (20) Chotkowski, M.; Czerwiński, A. *Electrochemistry of Technetium*; Monographs in  
465 Electrochemistry; Springer International Publishing: Cham, 2021. [https://doi.org/10.1007/978-3-](https://doi.org/10.1007/978-3-030-62863-5)  
466 [030-62863-5](https://doi.org/10.1007/978-3-030-62863-5).
- 467 (21) Chotkowski, M.; Czerwiński, A. Electrochemical and Spectroelectrochemical Studies of

- 468        Pertechnetate Electroreduction in Acidic Media. *Electrochim. Acta* **2012**, *76*, 165–173.  
469        <https://doi.org/10.1016/j.electacta.2012.04.123>.
- 470 (22) Chotkowski, M.; Czerwiński, A. Thin Layer Spectroelectrochemical Studies of Pertechnetate  
471        Reduction on the Gold Electrodes in Acidic Media. *Electrochim. Acta* **2014**, *121*, 44–48.  
472        <https://doi.org/https://doi.org/10.1016/j.electacta.2013.12.142>.
- 473 (23) Chotkowski, M.; Wrzosek, B.; Grdeń, M. Intermediate Oxidation States of Technetium in  
474        Concentrated Sulfuric Acid Solutions. *J. Electroanal. Chem.* **2018**, *814*, 83–90.  
475        <https://doi.org/10.1016/j.jelechem.2018.02.042>.
- 476 (24) Paquette, J.; Lawrence, W. E. A Spectroelectrochemical Study of the  
477        Technetium(IV)/Technetium(III) Couple in Bicarbonate Solutions. *Can. J. Chem* **1985**, *63* (Iv),  
478        2369–2373.
- 479 (25) Chatterjee, S.; Hall, G. B.; Johnson, I. E.; Du, Y.; Walter, E. D.; Washton, N. M.; Levitskaia, T.  
480        G. Surprising Formation of Quasi-Stable Tc(VI) in High Ionic Strength Alkaline Media. *Inorg.*  
481        *Chem. Front.* **2018**, *5* (9), 2081–2091. <https://doi.org/10.1039/c8qi00219c>.
- 482 (26) Kuznetsov, V. V.; Chotkowski, M.; Poineau, F.; Volkov, M. A.; German, K.; Filatova, E. A.  
483        Technetium Electrochemistry at the Turn of the Century. *J. Electroanal. Chem.* **2021**, *893* (April),  
484        115284. <https://doi.org/10.1016/j.jelechem.2021.115284>.
- 485 (27) Salaria, G. B. S.; Rulfs, C. L.; Elving, P. J. 456. Polarographic Behaviour of Technetium. *J. Chem.*  
486        *Soc.* **1963**, No. 0, 2479–2484. <https://doi.org/10.1039/JR9630002479>.
- 487 (28) Salaria, G. B. S.; Rulfs, C. L.; Elving, P. J. Polarographic and Coulometric Determination of  
488        Technetium. *Anal. Chem.* **1963**, *35* (8), 979–982. <https://doi.org/10.1021/ac60201a018>.
- 489 (29) Grassi, J.; Devynck, J.; Trémillon, B. Electrochemical Studies of Technetium at a Mercury  
490        Electrode. *Anal. Chim. Acta* **1979**, *107* (C), 47–58. [https://doi.org/10.1016/S0003-](https://doi.org/10.1016/S0003-2670(01)93194-0)  
491        2670(01)93194-0.
- 492 (30) Colton, R.; Dalziel, J.; Griffith, W. P.; Wilkinson, G. 15. Polarographic Study of Manganese,  
493        Technetium, and Rhenium. *J. Chem. Soc.* **1960**, No. 0, 71–78.  
494        <https://doi.org/10.1039/JR9600000071>.
- 495 (31) Colton, R.; Peacock, R. D. An Outline of Technetium Chemistry. *Q. Rev. Chem. Soc.* **1962**, *16*  
496        (4), 299–315. <https://doi.org/10.1039/QR9621600299>.
- 497 (32) Astheimer, L.; Schwochau, K. Zur Polarographie Des Technetiums: I. Gleichstrom- Und  
498        Wechselstrompolarographische Untersuchungen an Pertechnetat-Lösungen. *J. Electroanal.*  
499        *Chem.* **1964**, *8* (5), 382–389. [https://doi.org/https://doi.org/10.1016/0022-0728\(64\)80072-3](https://doi.org/https://doi.org/10.1016/0022-0728(64)80072-3).
- 500 (33) Poineau, F.; Fattahi, M.; Den Auwer, C.; Hennig, C.; Grambow, B. Speciation of Technetium and

- 501 Rhenium Complexes by in Situ XAS-Electrochemistry. *Radiochim. Acta* **2006**, *94* (5), 283–289.  
502 <https://doi.org/10.1524/ract.2006.94.5.283>.
- 503 (34) Ameer, Z. O.; Husein, M. M. Electrochemical Behavior of Potassium Ferricyanide in Aqueous  
504 and (w/o) Microemulsion Systems in the Presence of Dispersed Nickel Nanoparticles. *Sep. Sci.*  
505 *Technol.* **2013**, *48* (5), 681–689. <https://doi.org/10.1080/01496395.2012.712594>.
- 506 (35) Mayordomo, N.; Rodríguez, D. M.; Schild, D.; Molodtsov, K.; Johnstone, E. V.; Hübner, R.;  
507 Shams Aldin Azzam, S.; Brendler, V.; Müller, K. Technetium Retention by Gamma Alumina  
508 Nanoparticles and the Effect of Sorbed Fe<sup>2+</sup>. *J. Hazard. Mater.* **2020**, *388*, 122066.  
509 <https://doi.org/10.1016/j.jhazmat.2020.122066>.
- 510 (36) Brett, C. M. A.; Brett, A. M. O. *Electrochemistry : Principles, Methods, and Applications*; Oxford  
511 University Press, 1993.
- 512 (37) Brett, C. M. A.; Brett, A. M. O. *Electroanalysis*; Oxford University Press, 1998.
- 513 (38) Du, C.; Tan, Q.; Yin, G.; Zhang, J. 5 - Rotating Disk Electrode Method. In *Rotating Electrode*  
514 *Methods and Oxygen Reduction Electrocatalysts*; Xing, W., Yin, G., Zhang, J. B. Eds.; Elsevier:  
515 Amsterdam, 2014; pp 171–198. [https://doi.org/https://doi.org/10.1016/B978-0-444-63278-](https://doi.org/https://doi.org/10.1016/B978-0-444-63278-4.00005-7)  
516 [4.00005-7](https://doi.org/https://doi.org/10.1016/B978-0-444-63278-4.00005-7).
- 517 (39) Nightingale, E. R. Viscosity of Aqueous Sodium Perchlorate Solutions. *J. Phys. Chem.* **1959**, *63*  
518 (5), 742–743. <https://doi.org/10.1021/j150575a025>.
- 519 (40) Andraos, J. On the Propagation of Statistical Errors for a Function of Several Variables. *J. Chem.*  
520 *Educ.* **1996**, *73*, 150–154.
- 521 (41) Bard, A. J.; Parsons, R.; Jordan, J. *Standard Potentials in Aqueous Solution*; Marcel Dekker, Inc.:  
522 New York, 1985.
- 523 (42) Wang, X.; Tao, Z. Diffusion of <sup>99</sup>TcO<sub>4</sub><sup>-</sup> in Compacted Bentonite: Effect of PH, Concentration,  
524 Density and Contact Time. *J. Radioanal. Nucl. Chem.* **2004**, *260* (2), 305–309.  
525 <https://doi.org/10.1023/b:jrnc.0000027101.01834.1b>.
- 526 (43) Ben Said, K.; Fattahi, M.; Musikas, C.; Revel, R.; Abbé, J. C. The Speciation of Tc(IV) in Chloride  
527 Solutions. *Radiochim. Acta* **2000**, *88* (9–11), 567–571. [https://doi.org/10.1524/ract.2000.88.9-](https://doi.org/10.1524/ract.2000.88.9-11.567)  
528 [11.567](https://doi.org/10.1524/ract.2000.88.9-11.567).
- 529 (44) Lafuente, B.; Downs, R. T.; Yan, H.; Stone, N. The Power of Databases: The RRUFF Project. In  
530 *Highlights in Mineralogical Crystallography*; De Gruyter: Berlin, 2015; pp 1–30.
- 531 (45) Nakamoto, K. *Infrared and Raman Spectra of Inorganic and Coordination Compounds*; John  
532 Wiley & Sons, Inc.: Hoboken, NJ, USA, 2008. <https://doi.org/10.1002/9780470405840>.
- 533 (46) Weaver, J.; Soderquist, C. Z.; Washton, N. M.; Lipton, A. S.; Gassman, P. L.; Lukens, W. W.;

- 534 Kruger, A. A.; Wall, N. A.; Mccloy, J. S. Chemical Trends in Solid Alkali Pertechnetates. *Inorg.*  
535 *Chem.* **2017**, *56*, 2533–2544. <https://doi.org/10.1021/acs.inorgchem.6b02694>.
- 536 (47) Thomas, R. W.; Heeg, M. J.; Elder, R. C.; Deutsch, E. Structural (EXAFS) and Solution  
537 Equilibrium Studies on the Oxotechnetium(V) Complexes  $\text{TcO}_X4^-$  and  $\text{TcOX}_5^{2-}$  (X = Cl, Br).  
538 *Inorg. Chem.* **1985**, *24* (10), 1472–1477. <https://doi.org/10.1021/ic00204a014>.
- 539 (48) Schwochau, K.; Krasser, W. Schwingungsspektren und Kraftkonstanten der Hexahalogeno-  
540 Komplexe des Technetium(IV) und Rhenium(IV). *Zeitschrift für Naturforsch. A* **1969**, *24* (3),  
541 403–407. <https://doi.org/doi:10.1515/zna-1969-0316>.
- 542 (49) Gu, B.; Ruan, C. Determination of Technetium and Its Speciation by Surface-Enhanced Raman  
543 Spectroscopy. *Anal. Chem.* **2007**, *79* (6), 2341–2345. <https://doi.org/10.1021/ac062052y>.
- 544 (50) Mikelsons, M. V.; Pinkerton, T. C. Raman Spectroscopic Evidence for Tc-Oxo Cores in Tc-HEDP  
545 Complexes. *Int. J. Radiat. Appl. Instrumentation. Part* **1987**, *38* (7), 569–570.  
546 [https://doi.org/10.1016/0883-2889\(87\)90206-1](https://doi.org/10.1016/0883-2889(87)90206-1).
- 547 (51) *NIST X-Ray Photoelectron Spectroscopy Database, Version 4.1*; National Institute of Standards  
548 and Technology (NIST): Gaithersburg, USA, 2012.
- 549 (52) Beard, B. C. Sodium Salts of Chlorine Oxyacid Anions, Cl(+7), Perchlorate, XPS Comparison  
550 Spectra. *Surface science spectra.* **1993**, (2)2, 97–103. <https://doi.org/10.1116/1.1247738>.
- 551